


Role of modularity in self-organization dynamics in biological networksBram A. Siebert¹, Cameron L. Hall^{1,2}, James P. Gleeson¹, and Malbor Asllani¹¹*MACSI, Department of Mathematics and Statistics, University of Limerick, Limerick V94 T9PX, Ireland*²*Department of Engineering Mathematics, University of Bristol, Woodland Road, Clifton BS8 1UB, United Kingdom* (Received 26 March 2020; revised 10 July 2020; accepted 13 October 2020; published 11 November 2020)

Interconnected ensembles of biological entities are perhaps some of the most complex systems that modern science has encountered so far. In particular, scientists have concentrated on understanding how the complexity of the interacting structure between different neurons, proteins, or species influences the functioning of their respective systems. It is well established that many biological networks are constructed in a highly hierarchical way with two main properties: short average paths that join two apparently distant nodes (neuronal, species, or protein patches) and a high proportion of nodes in modular aggregations. Although several hypotheses have been proposed so far, still little is known about the relation of the modules with the dynamical activity in such biological systems. Here we show that network modularity is a key ingredient for the formation of self-organizing patterns of functional activity, independently of the topological peculiarities of the structure of the modules. In particular, we propose a self-organizing mechanism which explains the formation of macroscopic spatial patterns, which are homogeneous within modules. This may explain how spontaneous order in biological networks follows their modular structural organization. We test our results on real-world networks to confirm the important role of modularity in creating macroscale patterns.

DOI: [10.1103/PhysRevE.102.052306](https://doi.org/10.1103/PhysRevE.102.052306)**I. INTRODUCTION**

Patterns are macroscopic structures that are the distinctive mark of the self-organization in a system of microscopic interacting entities [1]. They are ubiquitous in nature and can be seen in the spots of a leopard's fur or the colored scales of a butterfly's wing [2]. In 1952, Alan Turing published his seminal work on pattern formation, *The Chemical Basis of Morphogenesis*, where he laid down an elegant and plausible theory that can be used to explain the formation of patterns [3]. Turing developed a simple model of pattern formation that established the minimal requirements for a biochemical system to self-organize. Turing's minimal system is composed of two "competing" chemicals, an activator and an inhibitor, which share the same spatial domain where they react and diffuse. Based on a diffusion-driven instability mechanism, today known as Turing instability, Turing showed that it is possible to explain and predict the growth of spatially inhomogeneous perturbations away from a spatially homogeneous steady state. These perturbations in concentration are later stabilized by nonlinearities in the system, yielding the celebrated Turing patterns. It can be shown that the right combination of short-range activation and long-range inhibition, caused by slowly diffusing activators and rapidly diffusing inhibitors, enables the pattern forming phenomenon [4].

Conventionally, an activator-inhibitor system is modelled using a set of reaction-diffusion equations that describe the evolution of the concentrations of activator and inhibitor throughout a continuous medium. These equations can readily be adapted to describe activator-inhibitor systems in

discrete systems such as regular lattices, and they have been used in this way to describe pattern formations in cellular tissues [4,5]. However, biological tissue often takes more complex forms, and the spatial support cannot always be adequately formulated via regular lattices. Inspired by the network structures of early stages of embryogenesis [6], ecological metapopulations [7], or coupled chemical reactors [8], researchers have extended the reaction-diffusion formalism to complex biological networks [5,9–15]. These discrete structures consist of graphs where the nodes usually represent the cells inside which reactions occur, and the edges usually represent the routes through which cells communicate by exchanging chemicals.

Hütt *et al.* [16] recently argued that the formalism of activator-inhibitor systems is relevant to the dynamical processes evolving in the brain [16]. The implementation of network tools for analyzing the brain's structure has been used since the first years of network science [17]. In their seminal work, Watts and Strogatz [17] studied the topology of the neuronal network of the nematode *C. elegans* and discovered that these networks possess a "small-world" property. In the literature, it has also been argued that many brain networks might be small-world networks [18–20]. It is widely accepted that the small-world property of brain connectomes should help the communication between neurons inside the brain by integrating multiple segregated sources of information [21].

A further property of brain networks is that they are often modular [18] so that the neurons can be segregated into communities (referred to as modules) where two neurons chosen at random from the same module are much more

likely to be connected than two neurons chosen at random from different modules. The functional role that the modularity of brain connections has been discussed from several perspectives. For example, due to the increased structural stability [21,22], the modularity might have been crucial in the evolution and development of the brain. According to [18,22] modular topology can also optimize the wiring cost in the case of spatial networks. A small number of long-range (and thus costly) connections reduces the diameter of the network, and allows the remaining nodes, now grouped into communities or modules, to form dense small world networks. Also, more compact segregation of neurons may contribute to the specialization of the neurons in their functional duties [21]. To ensure both a low shortest path length, and a high clustering coefficient, brain networks are organized in a strict hierarchical manner [18,23,24] where at the first level of the hierarchy sets of nodes (the modules) are connected to mimic a small-world topology and the same happens at the second level of hierarchy and so on, until the single node level. For a more detailed discussion of the role of the hierarchy in the pattern formation process see the Appendix.

More generally, modularity is a common topological property that naturally emerges in biological, ecological, and social scenarios where the different communities are associated with different functions of the system represented by the network as a whole [25]. There are many examples of this: in protein interaction networks, the proteins that share similar functions are grouped together in modules [26]; in metabolic networks, there are structural and functional communities corresponding to cycles or pathways [27]; and in citation networks, scientific papers are clustered according to their research topic [28]. In addition to these properties, in this paper, we propose a mathematical mechanism that highlights the role that modularity takes in self-organizing processes in biological networks.

Using the Turing theory of pattern formation, we show that spatially extended patterns can be triggered by the segregation of the nodes (neurons) in distinguishable communities. To formally analyze the chances of such networks self-organizing, we use a linear stability approach known in the literature as the dispersion relation [2]. We focus on modular networks, which in contrast to many other random networks, are characterized by a small spectral gap, i.e., a small distance of the second largest eigenvalue [29] of the Laplacian from the origin. Let us notice here that a small spectral gap is a characteristic also of large (dense) regular graphs; however, here we focus on random graphs. To anticipate some of the technical details, we discuss the key features of modular networks in the following paragraphs and outline how these affect pattern formation.

For modular networks, the Laplacian eigenvalues that may be responsible for the Turing instability can be split into two sets. In one set, we have the eigenvalues emerging due to the global modularity of the network, which we denote as “modular eigenvalues.” In Sec. III, we will show that when only this part of the spectrum is responsible for the instability, then the shape of the associated pattern follows that of the network in the sense that nodes belonging to the same modules have very similar concentrations of the species among themselves, but these concentrations are distinctly different from the concentrations in other modules. In contrast, if the instability is

caused by the remaining set of eigenvalues, which correspond to the local connectivity of nodes, here denoted as “nonmodular eigenvalues,” then all the nodes have (in principle) different concentrations making the pattern globally heterogeneous. In this later case, if the eigenvalues responsible for the instability are limited to the eigenvalues belonging to a single module, then the pattern will first emerge in that module.

We aim to create a bridge between the role of the structure in many biological networks with the dynamical activity therein. In particular, in our model, we explain how communities of biological entities (cells, individuals, etc.) can act as functional units in their corresponding biological systems. As a consequence, we argue that this approach can potentially be used in community detection methods [30–32] for networked biological systems where Turing patterns are known to exist. However, it is important to note that this method partitions the network in a similar fashion to the Fiedler partitioning. Therefore, it is possible to underestimate the total number of communities. Additionally, using pattern formation for community detection does not distinguish between functional communities and structural communities.

In this paper we begin in Sec. II with a description of the mathematical background of Turing patterns. This will lead us into a discussion as to why modularity is critical to the formation of patterns in Sec. II. We describe the different types of patterns which form in Sec. III, and show how increasing the modularity helps in the formation of patterns. Finally in Sec. IV we look for Turing patterns in some real world networks.

II. PATTERN FORMATION ON A NETWORKED SYSTEM

In a continuous domain, the most simple Turing mechanism is given in terms of reaction-diffusion equations that describe the evolution through time and space of the concentrations of two competing chemical species, called the activator [with concentration denoted $u(x, t)$] and the inhibitor [with concentration denoted $v(x, t)$] [2,3]. In general, an activator increases production of both itself and the inhibitor. The inhibitor, in turn, slows down the growth in the activator. When the spatial support is instead discrete, constituted by spatial patches (nodes) connected through communicating routes (links) the reaction-diffusion mechanism can be formulated using ODEs, instead of PDEs [5]. In general, a two-species reaction-diffusion model on a network of N nodes will take the form

$$\begin{aligned} \frac{du_i}{dt} &= f(u_i, v_i) + D_u \sum_j L_{ij} u_j, \quad \forall i = 1, \dots, N, \\ \frac{dv_i}{dt} &= g(u_i, v_i) + D_v \sum_j L_{ij} v_j, \quad \forall i = 1, \dots, N, \end{aligned} \quad (1)$$

where u_i and v_i represent the concentrations of activator and inhibitor, respectively, at node i ; f and g are nonlinear functions that describe the net production rates of activator and inhibitor, respectively; D_u and D_v are the diffusion coefficients of activator and inhibitor, respectively; and \mathbf{L} is the graph Laplacian operator. The entries L_{ij} of the graph Laplacian are defined by $L_{ij} = A_{ij} - k_i \delta_{ij}$, where \mathbf{A} is the adjacency matrix, k_i is the degree of node i , δ is the Kronecker delta and

where we do not sum over repeated indices. To understand the development of spatial patterns, we analyze the linear stability of the system starting from a homogeneous steady state (u^*, v^*) that is stable in the absence of diffusion. If the diffusion coefficients are nonzero and the ratio $\rho = D_v/D_u$ is large enough, the steady state (u^*, v^*) becomes unstable and small random perturbations of the previous steady state will grow. This growth is exponential in the initial linear regime, and may then be stabilized by the nonlinear terms of the functions f and g so that the system reaches a stable but spatially inhomogeneous steady state. Such a mechanism is responsible for the emergence of Turing patterns.

The linearized system in matrix form reads

$$\frac{d(\delta\mathbf{x})}{dt} = (\hat{\mathbf{J}} + \mathbf{D}\hat{\mathbf{L}})\delta\mathbf{x}, \quad (2)$$

where $\delta\mathbf{x} = (\mathbf{u} - u^*\mathbf{1}_N, \mathbf{v} - v^*\mathbf{1}_N)$ is the perturbations vector of the activator \mathbf{u} and inhibitor \mathbf{v} species, $\mathbf{1}_N$ is the all-ones N -dimensional vector, and

$$\mathbf{D} = \begin{bmatrix} D_u \mathbf{I}_N & 0 \\ 0 & D_v \mathbf{I}_N \end{bmatrix}$$

is the diffusion constant matrix. Note that \mathbf{I}_N represents the N by N identity matrix, so that \mathbf{D} is $2N$ by $2N$. The Jacobian matrix and the extended Laplacian are correspondingly

$$\hat{\mathbf{J}} = \begin{bmatrix} f_u \mathbf{I}_N & f_v \mathbf{I}_N \\ g_u \mathbf{I}_N & g_v \mathbf{I}_N \end{bmatrix}, \quad \hat{\mathbf{L}} = \begin{bmatrix} \mathbf{L} & 0 \\ 0 & \mathbf{L} \end{bmatrix}.$$

Note here that the notation \mathbf{J} will be reserved to identify the Jacobian of the 2×2 reactions matrix:

$$\mathbf{J} = \begin{bmatrix} f_u & f_v \\ g_u & g_v \end{bmatrix}.$$

We then look for solutions to Eq. (2) of the form

$$\begin{aligned} \delta\mathbf{u} &= \sum_{\alpha=1}^N b_{\alpha} e^{\sigma(\Lambda_{\alpha})t} \Phi^{\alpha}, \\ \delta\mathbf{v} &= \sum_{\alpha=1}^N c_{\alpha} e^{\sigma(\Lambda_{\alpha})t} \Phi^{\alpha}, \end{aligned} \quad (3)$$

where Λ_{α} , Φ^{α} are, respectively, the eigenvalues and eigenvectors of the Laplacian \mathbf{L} matrix, $\sigma(\Lambda_{\alpha})$ are the eigenvalues of the extended Jacobian $(\hat{\mathbf{J}} + \mathbf{D}\hat{\mathbf{L}})$, and α is the index term.

As will be seen in the following, the description of the linear solution through the eigenvectors of the Laplacian matrix will be essential in our analysis for the prediction of the modularity of final patterns. In fact, depending on which eigenvalues $\sigma(\Lambda_{\alpha})$ have positive real part, we can control the final shape of the pattern, as in Fig. 3.

Following the standard approach described by [2,5,9], we substitute the expansion of the perturbations into Eq. (2). This decomposes the extended Jacobian to a 2×2 matrix (for each index α) for which the eigenvalue problem needs to be solved

$$\mathbf{J}_{\alpha} = \begin{bmatrix} f_u + D_u \Lambda_{\alpha} & f_v \\ g_u & g_v + D_v \Lambda_{\alpha} \end{bmatrix}, \quad (4)$$

where subscripts on the activation function $f(u, v)$ and the inhibition function $g(u, v)$ represent partial derivatives evaluated at (u^*, v^*) . To study the stability of the linear system

we look for positive real parts of the eigenvalues of \mathbf{J}_{α} . Turing instability occurs when the real part of the larger of the two eigenvalues $\sigma(\Lambda_{\alpha}) = (\text{tr}\mathbf{J}_{\alpha} + \sqrt{(\text{tr}\mathbf{J}_{\alpha})^2 - 4\det\mathbf{J}_{\alpha}})/2$ is positive. The relation between the eigenvalues of the extended Jacobian and the eigenvalues of the Laplacian $\sigma(\Lambda_{\alpha})$ is known in the literature as the dispersion relation [2], for the continuous version see Appendix A 2. For an activator-inhibitor system the necessary conditions for stability are $\text{tr}\mathbf{J}_{\alpha} < 0$ and $\det\mathbf{J}_{\alpha} > 0$. The first condition is always true since $\text{tr}\mathbf{J}_{\alpha} = \text{tr}\mathbf{J} + (D_u + D_v)\Lambda_{\alpha}$, and this is negative since the stability of the fixed point in the absence of diffusion implies that $\text{tr}\mathbf{J} < 0$, while the nonpositivity of the Laplacian spectrum implies $\Lambda_{\alpha} < 0$. We therefore turn our attention to the second condition for stability, which concerns $\det\mathbf{J}_{\alpha} = \det\mathbf{J} + (f_u D_v + g_v D_u)\Lambda_{\alpha} + D_u D_v \Lambda_{\alpha}^2$. In order for a Turing instability to occur, we require $\det\mathbf{J}_{\alpha} < 0$. Noting that the stability of the fixed point in the absence of diffusion implies that $\det(\mathbf{J}) > 0$ and noting that $\Lambda_{\alpha} < 0$, it is straightforward to conclude that the only way for $\det\mathbf{J}_{\alpha}$ to be negative is for $(f_u D_v + g_v D_u)$ to be positive. Without loss of generality we define u to be the activator and v to be the inhibitor. Recalling the previous definition of an activator-inhibitor system, u increases the production of both species while v decreases the production of both species. As a result of this, the signs of the respective partial derivatives are $f_u > 0$, and $g_v < 0$. Therefore, we require $\rho = D_v/D_u > 1$ for instability [2,3,5], implying that the inhibitor should diffuse faster than the activator in order for Turing patterns to arise. In many practical cases, this difference needs to be very large to achieve $\det(\mathbf{J}_{\alpha}) < 0$.

Case for $D_v \gtrsim D_u$

From experimental observations [33–36] it is rarely true that the inhibitor diffuses much faster than the activator, but instead the chemicals diffuse with similar rates. In the case where $D_v \gtrsim D_u$, it can be shown that the dispersion relation is positive only for values of the spectrum of the Laplacian very near to the origin. To prove this we analyze the behavior of $\det(\mathbf{J}_{\alpha})$ when considered as a function of Λ_{α} ; more precisely, we focus on the value of Λ_{α} corresponding to a minimum of $\det(\mathbf{J}_{\alpha})$. It is known in the literature [2] that for the continuous case, there will always exist a nonpositive value of Λ_{α} such that $\det(\mathbf{J}_{\alpha}) < 0$ or, in other words, that Turing instability can occur. To proceed with our analysis, in the following, we will consider that Λ_{α} takes continuous values and will see that the spectrum of a (strongly) modular network fits in the domain of the continuous dispersion relation for which the instability occurs for the particular case $D_v \gtrsim D_u$. We start by differentiating with respect to Λ_{α} and after some algebraic manipulation, we find that the minimum of $\det\mathbf{J}_{\alpha}$ is found at $\Lambda_{\alpha} = \Lambda_{\min}$ where

$$\Lambda_{\min} = -\frac{f_u \rho + g_v}{2D_v}. \quad (5)$$

From relation (5) we note that if D_v is kept fixed while $\rho \rightarrow 1$ then $\Lambda_{\min} \rightarrow 0$. To show this we set $\rho = 1 + \epsilon$. Under the conditions of the Turing instability, Λ_{\min} is nonpositive, so $(1 + \epsilon)f_u + g_v > 0$. Rearranging, we can write $(1 + \epsilon)f_u + g_v = \text{tr}\mathbf{J} + \epsilon f_u$ and, noting that $\text{tr}\mathbf{J}$ is necessarily negative, we

conclude that the positive quantity $\text{tr}\mathbf{J} + \epsilon f_u$ can be at most of order ϵ since $\epsilon f_u > |\text{tr}\mathbf{J}|$. This shows that Λ_{\min} is of order ϵ . Therefore, as ϵ decreases, the value of Λ_α for which $\det\mathbf{J}_\alpha$ is at its minimum tends towards the origin. Hence, the possible values of Λ_α that may permit Turing instabilities tend towards zero as the ratio ρ of diffusivities tends to 1. In practice, this implies that the range of values of Λ_α for which instabilities can occur decreases in size and is restricted to small values of Λ_α . Therefore, a small spectral gap is needed to allow patterns to form. This is significant for the analysis of modular networks that follows since, as shown in the following section, modular networks are characterized by a small spectral gap $|\Lambda_2 - \Lambda_1|$. Hence the Laplacian of a modular network will have eigenvalues close to the origin. Because of this, we are able to find modular networks where Turing instabilities, and thus pattern formation, may occur where otherwise (i.e., in nonmodular networked systems) they would not. This modular pattern formation may even occur for values of ρ that are close to those observed in real systems.

III. TURING PATTERNS ON MODULAR NETWORKS

It has been argued that the existence of particular topological features in many types of networks, including brain networks, are of crucial importance in several important processes from neuronal communication [39] to structural robustness [40]. Such functional properties are based on the short average path length that characterizes this family of networks. We emphasized in the preceding subsection that the spectral gap is an important ingredient for the Turing instability. In this section, we further illustrate this fact by taking into account a special family of networks, the modular ones, that are known for their lack of spectral gap. As a comparison we contrast the process of pattern formation in a nonmodular network such as a Newman-Watts (NW) network (a particular case of a small-world network) with the pattern formation on a modular network generated using the stochastic block model (SBM).

As described in Refs. [18,21,41], modular structure has been identified in many brain networks. Since the FitzHugh-Nagumo model [42,43] is both useful for modeling neuronal dynamics [2], and since it can exhibit spatial pattern formation [2,11], we will use this model throughout this paper. In dimensionless form, FitzHugh-Nagumo dynamics correspond to using the functions $f(u, v) = u - u^3 - v$ and $g(u, v) = c(u - a + bv)$ to describe the net production of activator and inhibitor in Eq. (1) where a , b , and c are constants. The parameters of the model are always chosen such that we have a stable fixed point.

In Fig. 1 we compare the pattern on a single-module NW network (of 125 nodes and 660 edges) and a modular network with five communities, each with 25 nodes and a local Erdős-Rényi (ER) topology. As can be observed from the dispersion relation in Fig. 1(b), the distribution of the eigenvalues of the Laplacian matrix for the NW network, which shows a large spectral gap. This makes the Turing instability impossible for the given choice of parameters (including $\rho = 5.5$), since the instability (i.e., values of Λ corresponding to positive values of the continuous curve) is concentrated near the origin. We could potentially create an instability by significantly increas-

ing ρ , or optimize the rewiring to minimize the diameter. As $t \rightarrow \infty$, the FitzHugh-Nagumo models considered in this paper will tend to an equilibrium. One way to depict these equilibria is to plot the concentration of the activator species at long times. For the nonmodular network described above, this is shown in Fig. 1(a) and we see that the activator concentration is homogeneous across all nodes as expected.

In contrast to this, for a strongly modular topology the spectrum is divided into two distinct sets of eigenvalues. The first set is those nonzero eigenvalues near the origin (of which there are $M - 1$ where M is the number of the modules) and the second set is composed of all the remaining eigenvalues that are far from the origin [44]. We note that both the NW network and the modular network have the same number of nodes and edges, so the difference between the networks' spectra cannot be attributed to a difference in the number of nodes or in the average degree of these nodes. As already anticipated, we will refer to the first set of nonzero eigenvalues of the Laplacian matrix as the modular eigenvalues [for example, in Fig. 1(d) the first four nonzero eigenvalues]. In Fig. 1(d), we observe that the modular eigenvalues are sufficiently close to 0 and in the interval of possible values of the spectrum where the instability can develop; in Fig. 1(c) we see that this leads to a pattern in the activator concentrations at equilibrium.

To understand the reason why the spectrum of a modular network can be divided into two subsets we should first explain the reason behind the spectral gap in small-world networks. As mentioned earlier, the denomination "small-world" refers to a certain class of networks, one feature of which is the small average distance between nodes. In Ref. [45], Bojan showed that the absolute value of the second largest Laplacian eigenvalue $|\Lambda_2|$ is bounded below by $|\frac{4}{Nd}|$, where N is the number of nodes in the network and d is the diameter. This means that for a fixed value of the size N of the network, the lower bound of the spectral gap (equivalently, $|\Lambda_2|$) is larger when the diameter d is smaller; this prevents a nonmodular network (such as a NW network) having a smaller spectral gap than a modular network [46]. We want to emphasise that regular networks (e.g., rings) have a large diameter, too, having this way a small spectral gap. However, our focus here is on random networks which, apart from the modular ones, are characterised by a small diameter.

To further investigate how the spectral gap changes for different network topologies, we look at three different networks in Fig. 2. We create these networks in a simple way. First we divide our 125 nodes into five modules of nodes, and define the total number of intra-edges (connections within modules) and inter-edges (connections between modules). Then we allocate each module an equal number of intra-edges and inter-edges and randomly connect nodes within and between the modules, while avoiding double entries in both cases. If we define the number of intra-edges to be much larger than the number of inter-edges, then this process will yield a network with as strong modular structure. We describe three examples of these networks with increasing "modularity," where modularity is defined by the Q function described in Refs. [37,38]. We first look at an ER graph, as shown in Fig. 2(b). Notice that there is a large spectral gap in the corresponding dispersion relation, as shown in Fig. 2(a). By simply modifying

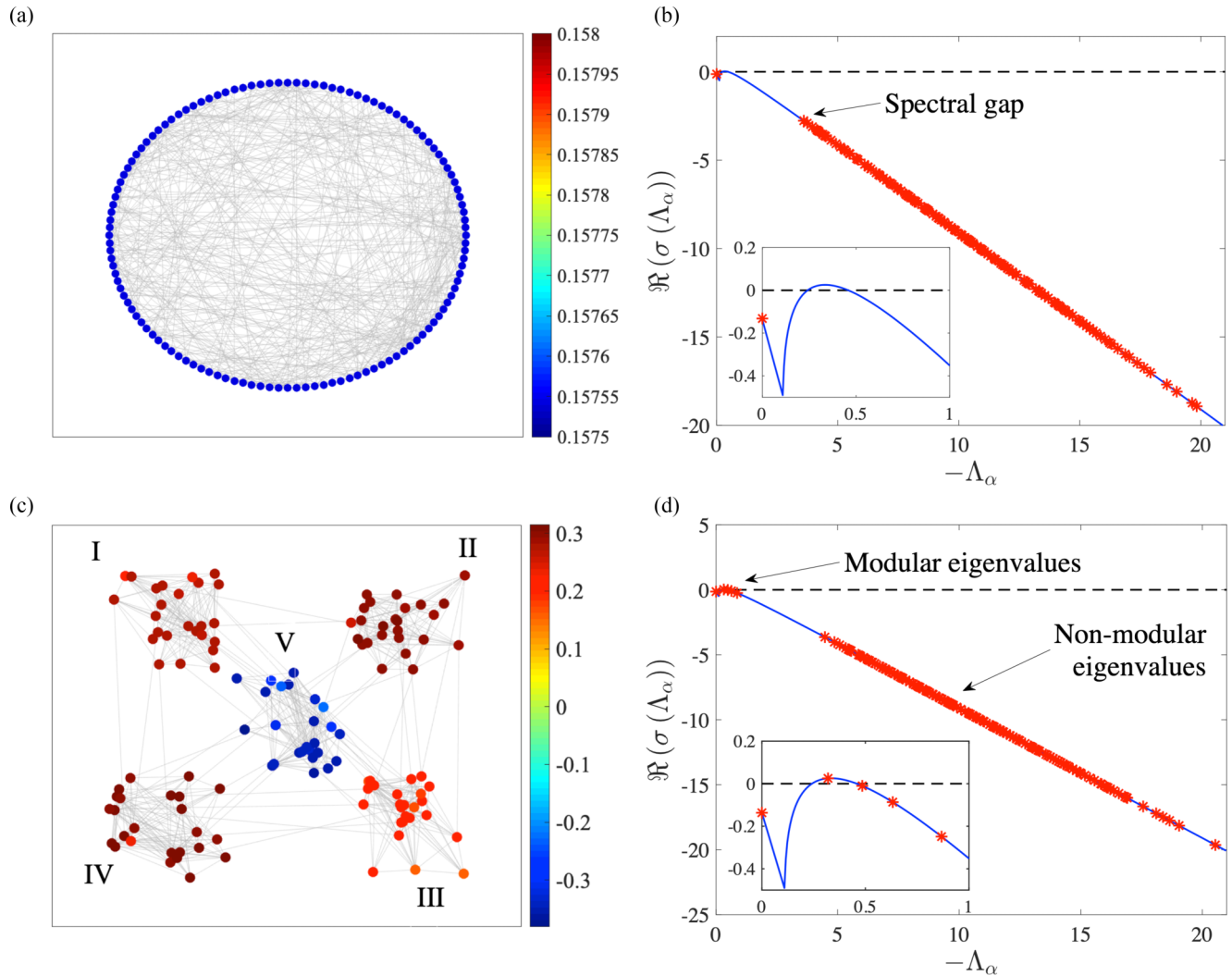


FIG. 1. Modular vs. nonmodular topology in Turing pattern formation. (a) A Newman-Watts (NW) network with $N = 125$ nodes, and 660 edges, where patterns are absent. The color of the nodes represents the concentration of the activator $u_i(t)$, at long time. (b) The dispersion relation of the NW network (red stars) overlain on the dispersion relation of the continuous case (blue curve), i.e., if the system was on a continuous domain and not on a network, where we substituted the eigenvalues of the Laplacian with a wave number k^2 . Notice the absence of the unstable eigenvalues (inset) and the gap between the zero eigenvalue and the second smallest Λ_2 , known as the spectral gap. (c) A modular network of the same size (same number of nodes and edges) as in (a) where indeed Turing patterns are present. The five modules are of the Erdős-Rényi (ER) family. The color of the nodes again represents the concentration of the activator $u_i(t)$ at long time. Note that the concentration of activator is homogeneous within modules, this is due to the modular nature of the network. (d) The dispersion relation of the modular network (red stars) overlain on the dispersion relation of the continuous domain (blue curve). Notice here the presence of unstable eigenvalues (inset) and that the eigenvalues are separated in two sets by an important gap, between the first and second set of eigenvalues. The first four nonzero eigenvalues are denoted as the modular eigenvalues and the remaining nonzero ones as the nonmodular eigenvalues. The parameters of the FitzHugh-Nagumo model are in both cases $D_u = 1$, $\rho = 5.5$, $a = 0.7$, $b = 0.05$, $c = 1.7$. Finally, note the different colormaps used between panels (a) and (c) to highlight the lack of patterns in the former.

the ratio of inter-edges to intra-edges, we can then generate a new network which begins to close the spectral gap, as in Figs. 2(c) and 2(d). Finally in Fig. 2(f) we have reduced the number of inter-edges such that patterns form, and the spectral gap is greatly decreased, as in Fig. 2(e). Notice again that there are two set of eigenvalues, the first four nonzero eigenvalues (which we refer to as modular eigenvalues) and the remaining nonmodular eigenvalues. This leads us to ask why a highly modular network closes the spectral gap so well. Note that in the Appendix, we consider the hierarchi-

cal case where each module is arranged in a small-world fashion.

To understand the small spectral gap of modular networks, we first imagine a scenario in which the modules are disconnected from each other. Individually, these modules are denser and smaller than the Newman-Watts network, therefore each of them is expected to have a relatively large spectral gap. From the algebraic connectivity theorem [47] we know that the number M of the connected components (the modules in this case) corresponds with the number of zero eigenval-

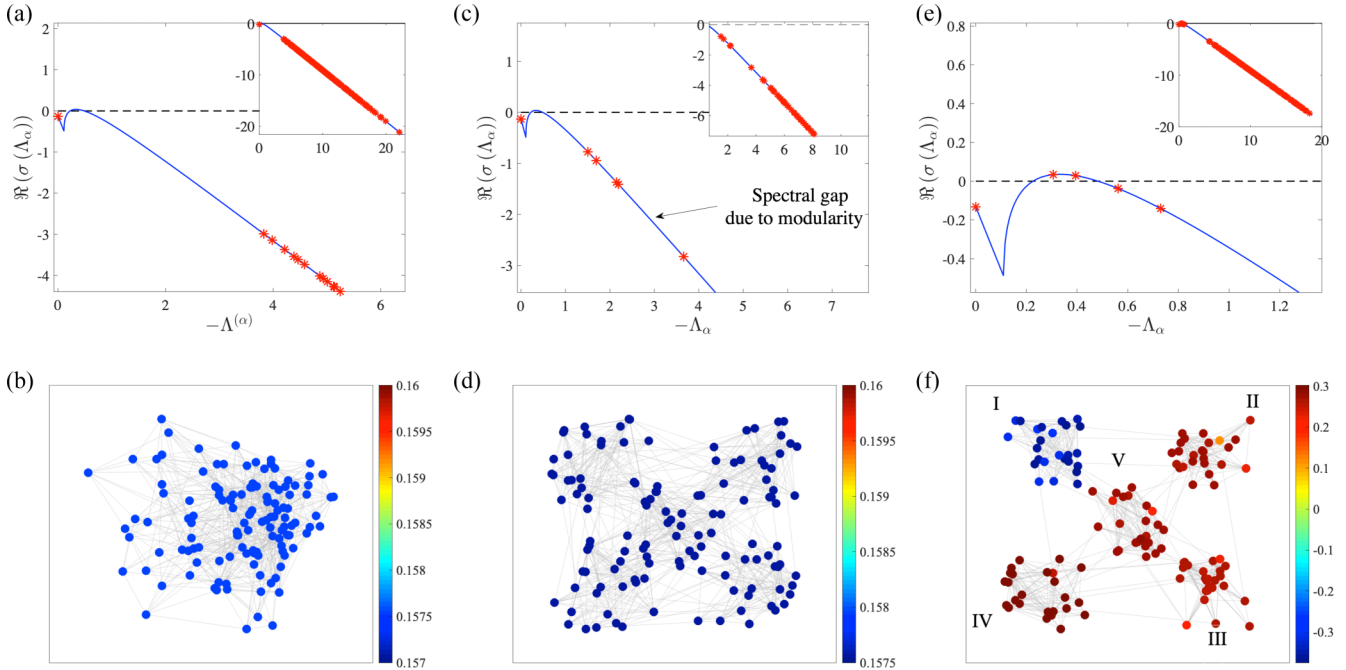


FIG. 2. Emergence of patterns by changing the modularity. (a) The dispersion relation for an ER network [shown in panel (b)], made of 125 nodes and 660 edges, and modularity measure $Q = 0.02562$. (c) The dispersion relation for a weakly modular network shown in panel (d) consisting of five modules and 540 intra-edges within modules, and 120 inter-edges between modules, and modularity $Q = 0.6150$. Notice that there is an emerging gap now between the first four nonzero eigenvalues and the rest of them. (e) The dispersion relation for a strongly modular network (f) with 630 intra-edges, 30 inter-edges, and $Q = 0.7545$. Notice that the spectral gap between the zero eigenvalue and the smallest nonzero eigenvalue is much smaller and a pattern has formed on the network. For all simulations $D_u = 1$, $\rho = 5.5$, $a = 0.7$, $b = 0.05$, and $c = 1.7$. Also we used the algorithms described in Refs. [37,38] with resolution parameter $\gamma = 1$ the modularity Q in each case.

ues of the Laplacian operator. However, once the modules are connected with a small number of links then $M - 1$ of these eigenvalues will move away from zero. From a spectrum perturbative analysis, we find that these become very small nonzero eigenvalues, with only one zero eigenvalue still remaining to signify that the whole modular network is connected [48]. Notice also that due to the algebraic connectivity, a network with a Laplacian spectral gap will always be modular. This explains the small size of the spectral gap in modular networks and consequently the emergence or not of Turing patterns, respectively, in small-world and modular networks [49,50].

We notice from Fig. 1(c) that although the pattern is highly heterogeneous at a global level, the patterns on nodes within each single module are quite homogeneous, having almost the same concentration of the species for each node in the module. Such macroscopic spatially extended patterns where densely connected entities (e.g., of biological nature) show the same amount of activity have been observed in different biological contexts [25–27] and in particular in dynamics of the brain [51,52]. While [51] is mainly an experimental paper, and first highlights the observation of spatial patterns on brain networks, we laid down a rigorous mathematical foundation that explores the importance of modularity to the formation of Turing patterns. Additionally, we here propose a self-organizing mechanism that explains the uniformity at the module level of Turing patterns in biological networks.

We can obtain insight into the patterns of u and v observed at equilibrium by constructing and analyzing the eigenvec-

tors associated with the Turing instabilities. From an initial condition close to the unstable homogeneous equilibrium, the rate of change in the concentrations u and v will initially be dominated by the eigenvector associated with the largest positive eigenvalue of the Jacobian. This initial growth will ultimately be stabilized by nonlinear terms, and we expect that the state equilibrium pattern of concentrations will be reminiscent of the eigenvectors associated with the instability [2,3]. To begin our analysis of the resultant patterns, we select parameters which lead to a single modular eigenvalue being positive, and observe the final “homogeneous by module” pattern as in Figs. 3(a)–3(c). The situation changes when the instability is exclusively induced from the nonmodular eigenvalues. In this case the concentration is no longer uniform for each module as shown in Figs. 3(d)–3(f). A hybrid state is obtained instead when both sets of eigenvalues contribute to the Turing instability as in Figs. 3(g)–3(i). These hybrid states can lead to patterns that are similar to either the modular patterns or the heterogeneous patterns. This is because the Turing instability in this case involves a competition between the eigenvectors associated with the unstable modular eigenvalues and the eigenvectors associated with the nonmodular eigenvalues. The dominant instability (and therefore the eigenvector that we expect to be most similar to the equilibrium pattern) will be the eigenvector associated with the largest eigenvalue of the Jacobian. In Fig. 3(h), for example, we observe that the largest eigenvalue of the Jacobian is associated with one of the modular eigenvalues of the Laplacian, and this is associated with a pattern

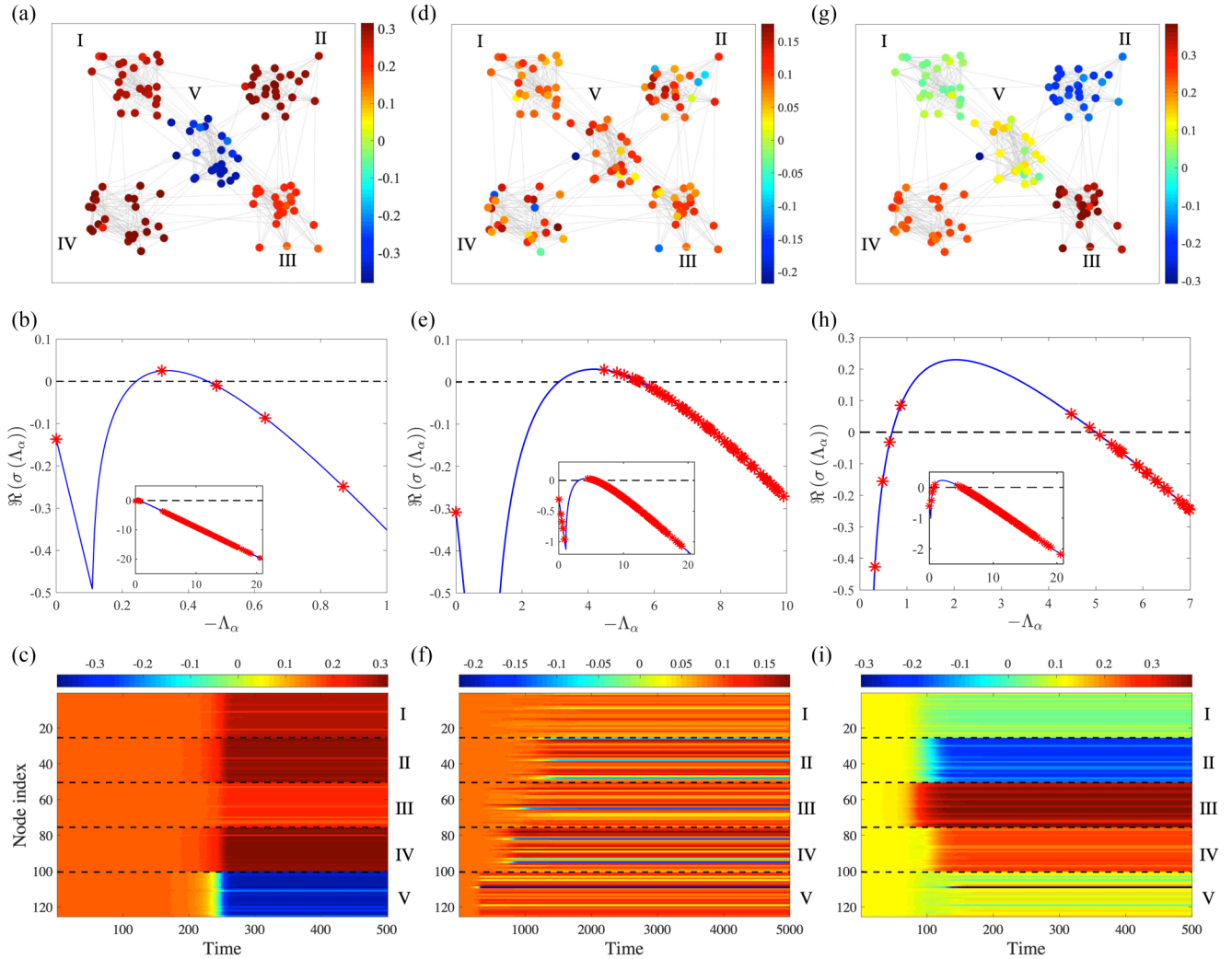


FIG. 3. Patterns classification on modular networks. In all the cases we used a network with $N = 125$ nodes, 660 edges, and a diameter of $d = 5$. (a) Modular patterns are formed when the concentration u_i is homogeneous across all nodes in the same module. (b) In the corresponding dispersion relation we fix the parameters in order to have a single positive modular eigenvalue. The parameters are $a = 0.7$, $b = 0.05$, $c = 1.75$, $\rho = 5.5$, $D_u = 1$. (c) Temporal evolution of the modular pattern. (d) A heterogeneous pattern emerges when the nodes inside the modules have different concentrations. (e) In the corresponding dispersion relation we fix the parameters in order to have a multiple positive nonmodular eigenvalues. The parameters are $a = 0.4$, $b = 0.05$, $c = 4.1$, $\rho = 14$, $D_u = 0.1$. (f) Temporal evolution of the heterogeneous pattern, in which one can see that the instability first developed in the central module. (g) In-between pattern is a mixed state of the previous patterns. (h) In this case the instability comes from the contribution of both modular and nonmodular eigenvalues. Here the parameters are $a = 0.6$, $b = 0.05$, $c = 3.625$, $\rho = 20$, $D_u = 0.16$. (j) Temporal evolution of the mixed pattern.

in Fig. 3(i) that could be described as almost being modular. In the Supplementary Material (SM) we discuss several criteria to establish which eigenvalue is dominating over the others [53].

To understand why the final shape of the pattern can be modular we focus on the study of the eigenvectors as plotted in Fig. 4. From the stability analysis we know that initially the pattern is shaped according to the unstable eigenvectors and this form is largely retained in the final nonlinear regime. Nevertheless, what surprises is the particular form of the eigenvectors associated with the modular eigenvalues as in Fig. 4(a); in particular, the fact that the components of the modular eigenvectors are segregated according to the respective modules [54]. To shed light on this peculiarity we will resort again to spectral graph theory.

As anticipated earlier, the smallest nonzero eigenvalue of the Laplacian Λ_2 defines the spectral gap known also in the literature as the Fiedler eigenvalue and defines the algebraic connectivity [55,56]. Its corresponding eigenvector is known as the Fiedler eigenvector and has the property that the entries of the nodes corresponding to the same modules take very similar values. Because of this property, the Fiedler eigenvector has been extensively used as the basis of several community detection methods [37,49,50]. However, it should be noted that the Fiedler partitioning can underestimate the total number of modules as we show in Fig. 4. The other modular eigenvectors also behave in a similar manner to the Fiedler eigenvector; their entries are segregated by module [49,50]. Since the modular eigenvectors are often the fastest growing modes in the Turing instability, this means that the

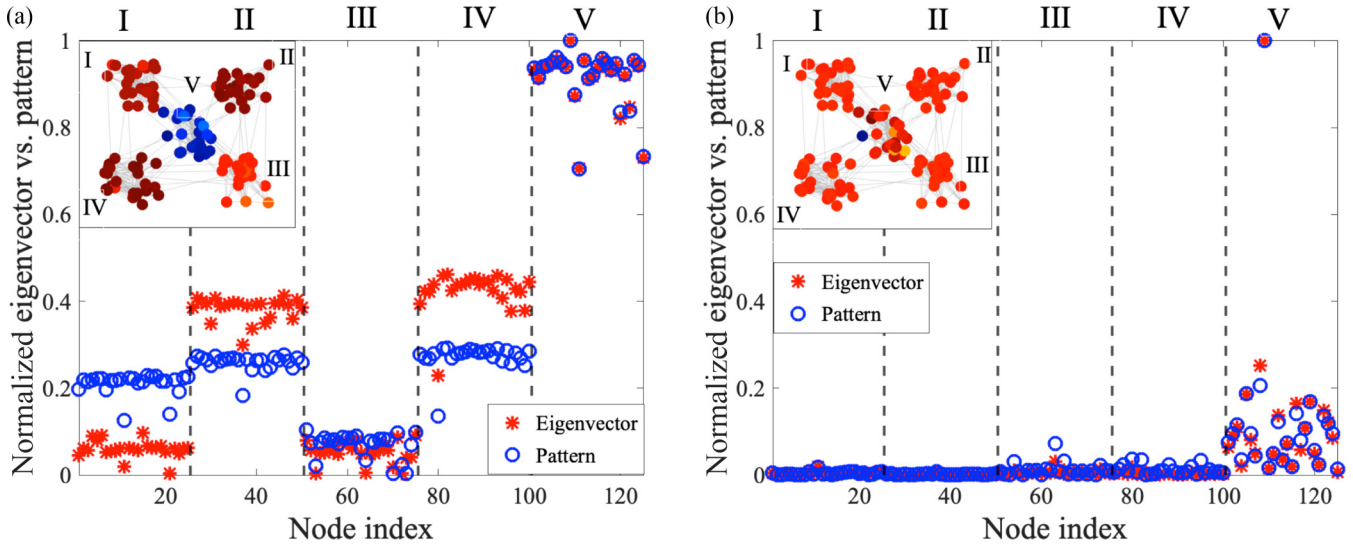


FIG. 4. Origin of modular patterns. In this figure, we plot the normalized patterns versus the normalized eigenvectors corresponding to a single positive modular and nonmodular eigenvalue, respectively. (a) A modular pattern (inset) is formed when one (or more) of the set of the modular eigenvalues is unstable and dominant over the nonmodular ones. The parameters are the same as in Fig. 3(a). (b) However, when the nonmodular eigenvalues dominate over the rest of the spectrum then heterogeneous patterns are created (inset). Furthermore in this setting it is also possible to identify the origin of instability from which the pattern first emerges, in this case the central module. The normalization for the patterns is simply $\frac{|u_i - u^*|}{\max_j |u_j - u^*|}$ for each entry i , and the same normalization is used for the eigenvector. Also the nodes are organized here in blocks of 25 individuals for each module. Finally the parameters for (b) are $D_u = 0.1$, $\rho = 13.38$, $a = 0.4$, $b = 0.05$, $c = 4$.

modular shape of the global pattern is a consequence of the modularity of the structure of the network itself.

On the other hand, when the instability is caused strictly by the nonmodular eigenvalues, another behavior occurs during the pattern forming phenomenon. This is best considered by again considering a modular network to be a perturbation of a network with initially M disconnected components. In such a case, each nonzero eigenvalue of the Laplacian will correspond to an eigenvector whose components are all zero outside a single component. A modular network will be a

small perturbation to this, and so the nonmodular eigenvectors will also be close to zero except within a single component. If only one nonmodular eigenvalue corresponds to a Turing instability, then only one module of the network will show pattern formation, as illustrated in Fig. 4(b). Thus, we can predict the module on which pattern formation will occur by looking at the components of the eigenvector whose eigenvalue corresponds to the fastest growing mode of the Turing instability.

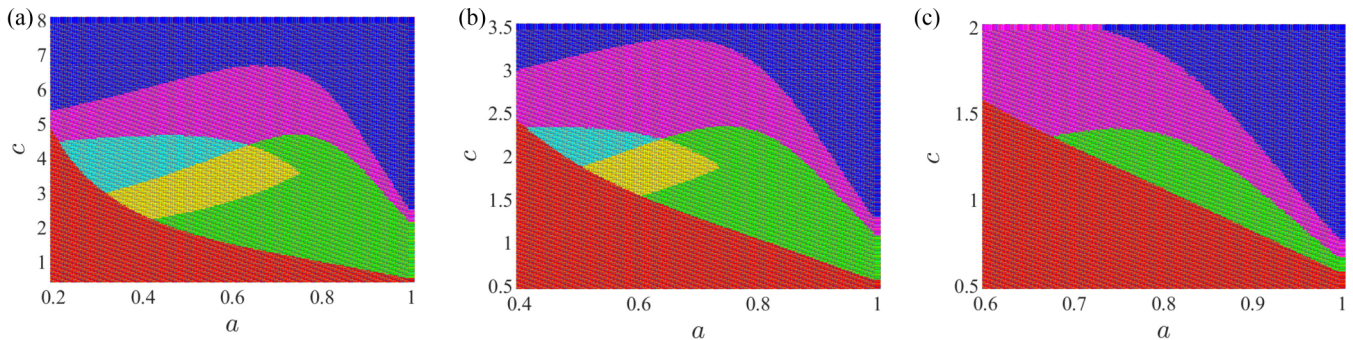


FIG. 5. Parameter space for decreasing diffusivities ratio. We classify different types of pattern on modular graphs in the parameter space of the (a), (c) FitzHugh-Nagumo model, a fixed value of $b = 0.05$, $D_u = 0.15$, and (a) $\rho = 20$, (b) $\rho = 10$, (c) $\rho = 6$. The portion of the parameter space indicated in red represents the region where no Turing patterns are allowed, as the system (in the absence of diffusion) is not in a steady state. All other regions correspond to parameters' sets for which Turing instability is allowed. The blue part is when the system is Turing stable, that is, the system is at a steady state but no Turing patterns form. The rest of the region is when patterns may occur: in the magenta region patterns only form in the continuous domain case, in green we have “modular” patterns, Fig. 3(a), yellow “mixed” state patterns, Fig. 3 (g), and cyan heterogeneous patterns, Fig. 3(d). Notice that as the ratio of diffusivities approaches 1, $\rho \rightarrow 1$, the only patterns which form are the modular patterns, showing that in a real scenario modularity is the only way to induce pattern formation in networks with modular structures, e.g., brain networks.

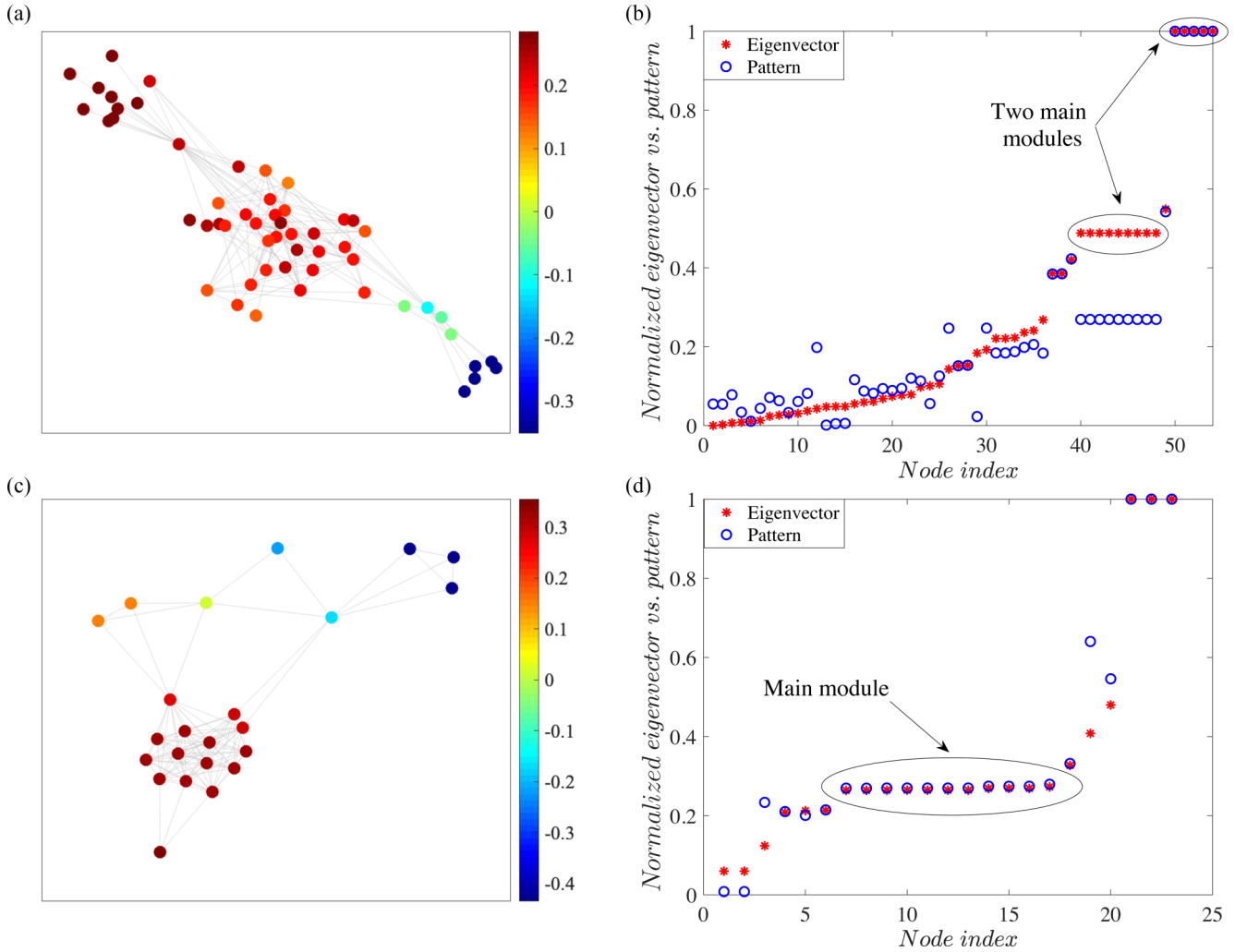


FIG. 6. Modular patterns on real-world networks. (a) The modular pattern of the neuronal network of 54 nodes of the nematode *P. Pacificus* [57] with parameters $D_u = 0.7$, $\rho = 4.5$, $a = 0.75$, $b = 0.04$, $c = 1.5$. (b) The comparison between the normalized unstable eigenvector and the final pattern shows the presence of two distinct modules. (c) The modular pattern of the network of 23 individuals (nodes) of a zebra herd [58] with parameters $D_u = 0.7$, $\rho = 4.5$, $a = 0.75$, $b = 0.04$, $c = 1.5$. (d) The comparison between the normalized unstable eigenvector and the final pattern shows the presence of a main module. Note that, to concentrate on the effects of modularity only, in both cases the networks were simplified to be undirected, and unweighted. We also extracted the giant component in each case.

So far we considered the contribution in the formation of patterns of both modular and nonmodular eigenvalues, however, when we deal with Turing patterns in real scenarios the ratio $\rho = D_v/D_u$ is quite close to one [33–36]. To evaluate the conditions under which different patterns form in real conditions we now explore the parameter space of the FitzHugh-Nagumo dynamics in more detail. Note that in order for a Turing pattern to form, we must begin from a stable fixed point.

In Fig. 5 it can be observed that although different types of patterns can be found in the space of the parameters a and c , as the ratio of diffusivities gets closer to 1 the region where patterns can occur shrinks and, more importantly, the only possible Turing patterns are modular ones (indicated in green color). One could find patterns in the other regions by tuning the diffusion parameters, except in the red region due to the absence of a stable fixed point.

The result that brain networks have optimized their spatial interaction matrix to allow pattern formation has been already claimed by experimental observers [51,52]; we present

a mechanism that explains the role of modularity in achieving this pattern formation.

IV. SELF-ORGANIZATION IN REAL MODULAR NETWORKS

Heretofore we discussed the role of modularity in the formation of patterns only for synthetic networks. In this part we will illustrate our findings in real examples of biological or ecological networks. The neuronal networks of several primitive animals such as nematodes have been well characterized. Indeed, it was the study of nematode neuronal networks that first inspired the development of small-world network models [17]. In Fig. 6(a) we show the final modular pattern of the nematode *P. pacificus* [57]. This follows from the theoretical prediction of the unstable Fiedler eigenvector, shown in Fig. 6(b). Here we used the Fiedler eigenvector to identify the communities of neurons [37]. In this particular case two modules are clearly distinguishable and the level of activity of the

nodes inside the modules are quite homogeneous. Other examples of Turing patterns in neuronal networks are presented in the Supplementary Material [53]. Although the modularity of brain networks has been well-studied [18,21,39,41] other types of natural networks manifest this property also. For instance, this is the case for ecological networks where the individuals are connected to each other through trophic relations [2,58]. Such modular contact networks have also been shown to be crucial for the pattern of disease spreading [59,60]. In Figs. 6(c) and 6(d) we present, respectively, the equilibrium pattern of the FitzHugh-Nagumo equations and its comparison to the unstable eigenvector of the contact network of a zebra herd [58] where a community of 11 individuals out of a total of 23 is clearly visible. However, the formation of patterns of spreading are not limited only to contact networks, which in general can be small in size. Modularity is a common property in other types of networks which, although they are not directly related to biological systems, are still essential for biological phenomena occurring on them. This is, for instance, the case for networks of human mobility, such the roads networks in the city of Chicago presented in the SM [53,61–64], which are decisive for the spreading of an epidemics in the entire urban area [59,60]. These examples all show agreement with the mathematical analysis we show so far.

V. DISCUSSION AND CONCLUSION

In this paper we analytically and numerically explored pattern formation on modular networks. We showed that modularity, a ubiquitous topological feature of many biological networks, is crucial for the self-organization of the global dynamics on a network. To study this behavior we considered here the Turing instability as a paradigmatic mechanism for pattern formation in biology, ecology, or neuroscience. The possibility of pattern formation via the Turing mechanism on nonmodular networks is limited to unrealistically extreme ratios of the diffusion constants of the activator and inhibitor species making the small spectral gap of the Laplacian matrix a fundamental requirement for the Turing instability. This feature is a structural advantage of modular networks which follows from spectral perturbation theory. A strongly modular network can be considered as a set of connected components weakly attached with a small number of intermodule links. From spectral perturbation theory this yields a number — equal to one fewer than the number of modules — of nonzero eigenvalues very near to the origin. This characterization at the linear stability level influences the shape of the spatially extended patterns. Due to the segregation of the entries of the eigenvectors corresponding to the set of modular eigenvalues, we are able to explain why Turing patterns are homogeneous per module on these networks.

This result opens to an important aspect regarding the functional resolution of the brain modes which was hypothesized [16,18,65] in several experimental observations [51,52]. The model we present here constitutes an alternative self-organizing mechanism where the modules are presented as functional blocks of biological networks. In this sense, we argue that the module is the smallest spatial unit to be taken into account from the functional point of view, i.e., if we

“zoom” out far enough from a modular network, the individual modules behave like individual supernodes. For the particular example of the brain the modules might be the supernodes of the functional connectomes [41,51,65]. Indeed, the (self)segregation of the network structure in modules [25] influences also the shape of the dynamical pattern on it. Based on the fact (see [16,18,41] and Fig. 6) that in real scenarios Turing patterns should be exclusively modular, we believe that the results we show here can be potentially used to formulate a community detection protocol [25,32,37] in the case where patterns of self-organized activity are known to exist.

In the case when we relax Turing conditions to allow the instability for the nonmodular part of the spectrum, then we can use the eigenvector corresponding to the largest eigenvalue to indicate the module in which the Turing pattern is first seeded before finally spreading to the rest of the network. This behavior can potentially make the pattern formation process a powerful diagnostic tool for studying and eventually controlling the emergence of abnormal dynamics which characterize many neurological diseases [66] or the spread of an epidemic in a group of individuals [59,60]. We test our theoretical results on several real connection data sets of neuronal, ecological, and infrastructure networks verifying the correctness of our findings, that modularity is crucial for the development of patterns, and that when the instability is derived from the first set of modular eigenvalues, that the resultant self-organization follows the modular structure of the network.

The results we presented here can extend also to more complicated scenarios. This is, for example, the case when the hierarchy of a network is considered as a complement to its modularity. In the Appendix we show that in a hierarchical modular network the modular eigenvalues are even more relevant for the Turing pattern forming process. Further extensions of our approach are also possible; for example, to consider the effect of directed edges in a modular network. In this case we expect a richer dynamics where traveling Turing waves should emerge in a directed modular networks [11].

ACKNOWLEDGMENTS

B.A.S. acknowledges funding from the Irish Research Council under Grant No. GOIPG/2018/3026. The work of J.P.G. and M.A. is partly funded by Science Foundation Ireland (Grants No. 16/IA/4470, No. 16/RC/3918, No. 12/RC/2289 P2, and No. 18/CRT/6049) and cofunded under the European Regional Development Fund.

APPENDIX

1. FitzHugh-Nagumo model

We used the Fitzhugh-Nagumo model throughout this paper [42,43], which is one of the first and best-known mathematical models used to describe the spiking dynamics of neurons. In terms of mathematical equations the behavior of a single neuron is described by

$$\begin{aligned}\frac{du}{dt} &= u - u^3 - v, \\ \frac{dv}{dt} &= c(u - av - b),\end{aligned}\tag{A1}$$

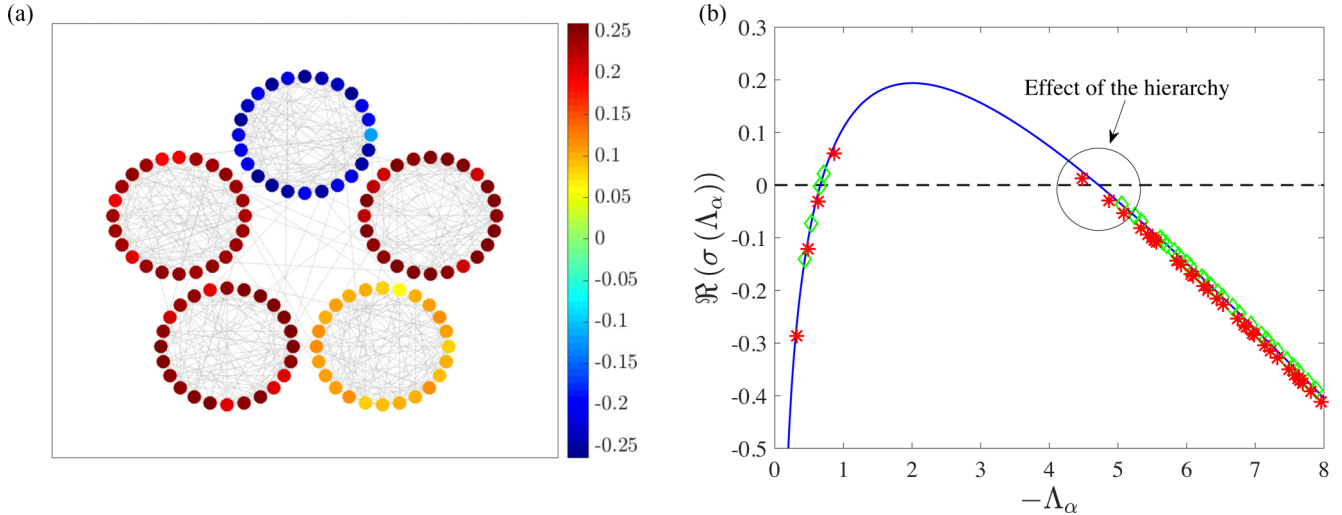


FIG. 7. Patterns on hierarchical modular networks. (a) The modular pattern on five connected Newman-Watts networks, each with $N = 25$ nodes and 125 edges. Each module is connected to its clockwise and counterclockwise neighbors with two random edges. There are a further 25 random edges added to induce shortcuts, as in the Newman-Watts style. (b) The dispersion relation of the hierarchical network (green diamonds) and modular network with random (ER) modules (red stars) with the same number with $D_u = 0.15$, $\rho = 17$, $a = 0.7$, $b = 0.05$, $c = 3.625$. The larger gap between the first five eigenvalues and the rest arises due to the hierarchy of the network.

where u is the membrane potential and v the recovery variable. The model itself was first introduced by FitzHugh [42] to explain the generation of spikes in excitable systems, i.e., neurons. A spike is a short-lasting elevation of the membrane voltage u diminished over time by a slower and linear recovery variable v once the system is periodically excited by an external current. The following year Nagumo *et al.* [43] developed the electric circuit which mimics such behavior. However, although the model itself is mainly used to describe the oscillatory behavior of neurons, it also admits a stable fixed point, which is a necessary requirement for Turing instabilities. Once this model is equipped with a diffusion term, it turns out to be a perfect candidate for pattern formation [2]. In recent years, with the rapid development of network science, the FitzHugh-Nagumo model has been extended to diffusively coupled networks [11,67].

2. Continuous Formulation

The original continuous framework for pattern formation, in one dimension, is

$$\begin{aligned} \frac{\partial u}{\partial t} &= f(u, v) + D_u \frac{\partial^2 u}{\partial x^2}, \\ \frac{\partial v}{\partial t} &= g(u, v) + D_v \frac{\partial^2 v}{\partial x^2}, \end{aligned} \quad (\text{A2})$$

where notation is as in Sec. II. The derivation of Turing patterns follows the same process as we describe in the main text, except in a continuous form. Of note, the extended Jacobian is now

$$\mathbf{J}_k = \mathbf{J} - \mathbf{D}k^2 = \begin{bmatrix} J_{11} - k^2 D_u & J_{12} \\ J_{21} & J_{22} - k^2 D_v \end{bmatrix}, \quad (\text{A3})$$

where k is the wave number. Then, the continuous dispersion relation, $\sigma(k)$, is plotted against the wave number, k^2 instead of the eigenvalues of the Laplacian.

3. Role of hierarchy of the brain networks in the pattern formation

We discussed the role that modularity has on pattern formation, isolating it from other topological features, which is, in fact, an integral aspect of many networks, including brain networks. So then a question that arises naturally is, how does the brain cope with maintaining both features and their functional properties at the same time? We now are able to answer this question by recalling an important empirical result that characterizes most real networks, their hierarchical structure [18,32,68]. In fact, most of the connectomes studied are organized in a modular structure, however, each module is further organized in a small-world fashion. This is another amazing observation how nature tends to self-organize to better optimize the benefit from the both structural features, the modularity and the small-worldness. In a hierarchical modular network the entire network is organized in modules which are attached to each other so as to have a small diameter and at the same time the nodes in the modules are connected in such way to form submodules again minimizing their diameter and this process goes on this way up to smallest building unity, the single nodes. A hierarchical structure stresses once more the necessity of modularity for the self-organizing phenomena in the networks. In Fig. 7 we show that the difference of the smallest nonmodular eigenvalue from the origin is larger when the modules have a small-world topology compared to when they are organized at random (e.g., ER network) for the same number of nodes, edges and modules. The reason for this can be found once more by taking a perturbative approach. The spectral gap of an individual module (disconnected from the rest of the network) is larger when its diameter is smaller, as it is in the Newman-Watts network used in Fig. 7.

Thus, in the presence of hierarchy, the cyan and the yellow regions in Fig. 5 would be even smaller making the modularity region shown in green larger compared to the previous two.

We notice, however, that the instability invariance is still valid for values of the diffusivities ratio ρ near to 1, that is when only the green region in the parameter space is available. In conclusion, a hierarchical arrangement where each module

is arranged in a small-world fashion, and these modules are again connected in a small-world fashion, are even better candidates for forming modular patterns than the modular networks studied in the main text.

-
- [1] G. Nicolis and I. Prigogine, *Self-Organization in Nonequilibrium Systems. From Dissipative Structures to Order Through Fluctuations* (Wiley, New York, 1977).
- [2] J. D. Murray, *Mathematical Biology II : Spatial Models and Biomedical Applications* (Springer-Verlag, Berlin, 2001).
- [3] A. M. Turing, *Bull. Math. Biol.* **52**, 153 (1990).
- [4] A. Gierer and H. Meinhardt, *Kybernetik* **12**, 30 (1972).
- [5] H. G. Othmer and L. E. Scriven, *J. Theor. Biol.* **32**, 507 (1971).
- [6] R. Schnabel, M. Bischoff, A. Hintze, A.-k. Schulz, A. Hejnl, H. Meinhardt, and H. Hutter, *Dev. Biol.* **294**, 418 (2006).
- [7] M. D. Holland and A. Hastings, *Nature* **456**, 792 (2008).
- [8] W. Horsthemke, K. Lam, and P. K. Moore, *Phys. Lett. A* **328**, 444 (2004).
- [9] H. Nakao and A. S. Mikhailov, *Nat. Phys.* **6**, 544 (2010).
- [10] M. Asllani, D. M. Busiello, T. Carletti, D. Fanelli, and G. Planchon, *Phys. Rev. E* **90**, 042814 (2014).
- [11] M. Asllani, J. D. Challenger, F. S. Pavone, L. Sacconi, and D. Fanelli, *Nat. Commun.* **5**, 4517 (2014).
- [12] M. Asllani, D. M. Busiello, T. Carletti, D. Fanelli, and G. Planchon, *Sci. Rep.* **5**, 12927 (2015).
- [13] M. Asllani, T. Carletti, and D. Fanelli, *Eur. Phys. J. B* **89**, 260 (2016).
- [14] R. Muolo, M. Asllani, T. Carletti, D. Fanelli, and P. K. Maini, *J. Theor. Biol.* **480**, 81 (2019).
- [15] M. Asllani, T. Carletti, D. Fanelli, and P. K. Maini, *Eur. Phys. J. B* **93**, 135 (2020).
- [16] M.-T. Hütt, M. Kaiser, and C. C. Hilgetag, *Philos. Trans. R. Soc. B* **369**, 1653 (2014).
- [17] D. Watts and S. Strogatz, *Nature* **393**, 440 (1998).
- [18] D. Meunier, R. Lambiotte, and E. T. Bullmore, *Front. Neurosci.* **4**, 200 (2010).
- [19] L. Harriger, M. P. V. D. Heuvel, and O. Sporns, *PLoS One* **7**, e46497 (2012).
- [20] J. D. Hahn, O. Sporns, A. G. Watts, and L. W. Swanson, *Proc. Natl. Acad. Sci.* **116**, 8018 (2019).
- [21] O. Sporns, *Networks of the Brain* (MIT Press, Cambridge, MA, 2010).
- [22] H. A. Simon, *Proc. Am. Philos. Soc.* **106**, 467 (1962).
- [23] O. Sporns, C. J. Honey, and R. Kötter, *PLoS One* **2**, e1049 (2007).
- [24] E. Bullmore and O. Sporns, *Nat. Rev. Neurosci.* **10**, 186 (2009).
- [25] M. Girvan and M. E. Newman, *Proc. Natl. Acad. Sci. USA* **99**, 7821 (2002).
- [26] F. Luo, Y. Yang, C.-F. Chen, R. Chang, J. Zhou, and R. H. Scheuermann, *Bioinformatics* **23**, 207 (2007).
- [27] H. Jeong, B. Tombor, R. Albert, Z. N. Oltvai, and A.-L. Barabási, *Nature* **407**, 651 (2000).
- [28] S. Redner, *Eur. Phys. J. B* **4**, 131 (1998).
- [29] The definition of the spectral gap depends on the way one defines the Laplacian matrix [32]. In our case the spectrum of the Laplacian is nonpositive.
- [30] S. Fortunato, *Phys. Rep.* **486**, 75 (2010).
- [31] M. E. Newman and M. Girvan, *Phys. Rev. E* **69**, 026113 (2004).
- [32] M. E. J. Newman, *Networks: An Introduction*, 2nd ed., (Oxford University Press, New York, 2018).
- [33] J. A. Vastano, J. E. Pearson, W. Horsthemke, and H. L. Swinney, *Phys. Lett. A* **124**, 320 (1987).
- [34] J. E. Pearson and W. Horsthemke, *J. Chem. Phys.* **90**, 1588 (1989).
- [35] V. Castets, E. Dulos, J. Boissonade, and P. De Kepper, *Phys. Rev. Lett.* **64**, 2953 (1990).
- [36] I. S. J. Horváth and P. D. Kepper, *Science* **324**, 772 (2009).
- [37] M. E. J. Newman, *Phys. Rev. E* **74**, 036104 (2006).
- [38] J. Reichardt and S. Bornholdt, *Phys. Rev. E* **74**, 016110 (2006).
- [39] O. Sporns and J. D. Zwi, *Neuroinformatics* **2**, 145 (2004).
- [40] R. Albert and A. L. S. Barabási, *Rev. Mod. Phys.* **74**, 47 (2002).
- [41] O. Sporns, D. R. Chialvo, M. Kaiser, and C. C. Hilgetag, *Trends Cognit. Sci.* **8**, 418 (2004).
- [42] R. FitzHugh, *Biophys. J.* **1**, 445 (1961).
- [43] J. Nagumo, S. Arimoto, and S. Yoshizawa, *Proc. IRE* **50**, 2061 (1962).
- [44] T. P. Peixoto, *Phys. Rev. Lett.* **111**, 098701 (2013).
- [45] B. Mohar, in *Proceedings of the Sixth Quadrennial International Conference on the Theory and Applications of Graphs*, edited by Y. Alavi, G. Chartrand, O.R. Oellermann, and A.J. Schwenk (Wiley, New York, 1991).
- [46] We want to emphasize that regular networks (e.g., rings) have a large diameter also, having this way a small spectral gap. However, our focus here is on random networks which, apart from the modular ones, are characterized by a small diameter.
- [47] G. H. Golub and C. F. van Loan, *Matrix Computations*, 3rd ed., (Johns Hopkins University Press, Baltimore, MD, 1996).
- [48] Notice also that due to the algebraic connectivity, a network with a Laplacian spectral gap will always be modular.
- [49] L. Donetti and M. A. M. Muñoz., *J. Stat. Mech.: Theor. Exp.* (2004) P10012.
- [50] E. Andreotti, D. Remondini, G. Servizi, and A. Bazzani, *Linear Algebra Appl.* **544**, 206 (2018).
- [51] G. B. Smith, B. Hein, D. E. Whitney, D. Fitzpatrick, and M. Kaschube, *Nat. Neurosci.* **21**, 1600 (2018).
- [52] P. L. Baniqued, C. L. Gallen, M. W. Voss, A. Z. Burzynska, C. N. Wong, G. E. Cooke, K. Duffy, J. Fanning, D. K. Ehlers, and E. A. Salerno, *Front. Aging Neurosci.* **9**, 426 (2018).
- [53] See Supplemental Material at <http://link.aps.org/supplemental/10.1103/PhysRevE.102.052306> for more information on these criteria.
- [54] Notice here that it may be, as in the case of Fig. 4, that different modules might share by chance the same level of components. However, this should not be understood as these entries belonging to the same module.

- [55] R. Schnabel, M. Bischoff, A. Hintze, A.-k. Schulz, A. Hejnol, H. Meinhardt, and H. Hutter, *Czech. Math. J.* **23**, 298 (1973).
- [56] F. Chung., *Spectral Graph Theory* (American Mathematical Society, Providence, RI, 1997).
- [57] D. J. Bumbarger, M. Riebesell, C. Rödelsperger, and R. J. Sommer, *Cell* **152**, 109 (2013).
- [58] S. R. Sundaresan, I. R. Fischhoff, J. Dushoff, and D. I. Rubenstein, *Oecologia* **151**, 140 (2006).
- [59] G. Sun, *Nonlinear Dyn.* **69**, 1097 (2012).
- [60] G. Sun, M. Jusup, Z. Jin, Y. Wang, and Z. Wang, *Phys. Life Rev.* **19**, 43 (2016).
- [61] <https://icon.colorado.edu/#!/networks>.
- [62] R. W. Eash, K. S. Chon, and D. E. Boyce, *Transp. Res. Rec.* **994**, 30 (1983).
- [63] D. E. Boyce, K. S. Chon, M. E. Ferris, Y. J. Lee, K.-T. Lin, and R. W. Eash, *Implementation and Evaluation of Combined Models of Urban Travel and Location on a Sketch Planning Network* University of Illinois, Urbana, and Chicago Area Transportation Study, xii + 169 (1985).
- [64] J. Kunegis, in *Proceedings of the 22nd International Conference on World Wide Web Companion, Rio De Janeiro* (ACM Digital Library, 2013), pp. 1343–1350.
- [65] O. Sporns and R. F. Betzel, *Annu. Rev. Psychol.* **67**, 613 (2016).
- [66] M. Asllani, P. Expert, and T. Carletti, *PLoS Comput. Biol.* **14**, e1006296 (2018).
- [67] M. Perc, *New J. Phys.* **7**, 252 (2005).
- [68] E. B. Ravasz and A. L. S. Barabási, *Phys. Rev. E* **67**, 026112 (2003).